

## Two-Dimensional Multiphase Behavior Induced by Sterically Hindered Conformational Optimization of Phenoxy-Substituted Phthalocyanines

Tomas Samuely,<sup>†</sup> Shi-Xia Liu,<sup>\*,‡</sup> Nikolai Wintjes,<sup>†</sup> Marco Haas,<sup>‡</sup> Silvio Decurtins,<sup>‡</sup> Thomas A. Jung,<sup>\*,§</sup> and Meike Stöhr<sup>\*,†</sup>

*Institute of Physics, University of Basel, Klingelbergstrasse 82, 4056 Basel, Switzerland, Department of Chemistry and Biochemistry, University of Bern, Freiestrasse 3, 3012-Bern, Switzerland, and Laboratory for Micro- and Nanostructures, Paul-Scherrer-Institute, 5232 Villigen, Switzerland*

*Received: November 14, 2007; In Final Form: January 23, 2008*

Symmetrically substituted phthalocyanines (Pcs) with eight peripheral di-(tert-butyl)phenoxy (DTPO) groups self-organize on Ag(111) and Au(111) substrates into various assembly structures. These different structural phases were studied by scanning tunneling microscopy (STM). On the basis of high-resolution STM images, molecular models are provided for each phase that account for the observed unequal surface densities. Notably, the specificity of the studied Pc derivative featuring the peripheral phenoxy groups remarkably increases its conformational possibilities. Particularly, the rotational degrees of freedom allow all the DTPO substituents to be arranged above the plane of the Pc core, forming a bowl-like structure, which in turn enables the interaction of the Pc core with the metal substrate. The proximity of the Pc core to the metal substrate together with the steric entanglement between neighboring DTPO substituents causes significant retardation of the thermodynamic optimization of the conformations.

### Introduction

Phthalocyanine (Pc) molecules have been extensively studied,<sup>1</sup> mainly because of their exceptional thermal and chemical stability but also because of their unique physical properties, namely their semiconducting behavior and tunable optical absorption features. In its most general sense, it is the delocalized  $\pi$ -electron system of the planar Pc skeleton, similar to porphyrins,<sup>2</sup> that makes phthalocyanines useful in different areas of materials science. Pcs have been effectively incorporated as active components in semiconductor devices, information storage systems, liquid crystal color displays, etc.<sup>3</sup> In the context of this report, these conjugated  $\pi$ -electron systems were studied as potential building blocks for supramolecular assemblies on different substrates. There are numerous examples of Pc-containing self-organized layers, whereby different metal ions are coordinated to the central Pc cavity, which have been investigated by means of scanning tunneling microscopy (STM) under a range of conditions. For example, FePc, CoPc, NiPc, and CuPc on Au(111) substrates<sup>4–7</sup> and CuPc and SnPc on Ag(111) substrates<sup>8,9</sup> were investigated under ultrahigh vacuum (UHV) conditions. Other notable examples are the well-defined adlayers of CoPc, CuPc, and ZnPc that were prepared on Au(111) by immersing the substrate into a benzene solution saturated with the molecules and then were studied by means of electrochemical STM.<sup>10–12</sup>

However, to considerably affect or even control the organization of the Pcs on a particular substrate further chemical and structural modifications other than varying the central atom of

the Pc core are necessary. For instance, subphthalocyanines<sup>13,14</sup> as well as naphthalocyanines<sup>15,16</sup> are such Pc analogues that exhibit a different two-dimensional (2D) molecular arrangement on substrates compared to original Pcs. Another very effective approach to change the architectural structures of Pc layers is to peripherally functionalize the molecules with various substituents. In particular, a large variety of chemical substituents can be attached to the macrocyclic core. By this method, numerous derivatives of the Pc family have been created by varying the number, type, length, and position of flexible side-chains, including linear or branched alkyl and alkoxy chains,<sup>17</sup> alkoxyphenoxy and alkylphenoxy substituents,<sup>18</sup> or even by annulating heterocycles to the periphery of the macrocycle.<sup>19</sup> Therefore, 2D ordered patterns of Pcs substituted with alkyl chains,<sup>20</sup> halogen atoms,<sup>21–23</sup> and other diverse substituents<sup>24</sup> were analyzed. Furthermore, similar to Pcs, porphyrins have also been used as a core entity for chemical functionalization to gain further supramolecular building blocks.<sup>25–28</sup>

In this paper, we report on a novel and complex phase behavior of specific Pc derivatives adsorbed on metallic substrates, and we discuss the physicochemical properties of such self-organized molecular monolayers. The actual Pc-DTPOs are symmetrically octasubstituted with di-(tert-butyl)phenoxy (DTPO) groups<sup>18c</sup> and contain either two H atoms or a Zn atom in the central cavity (Scheme 1). The DTPO substituents are similar to di-(tert-butyl)phenyl (DTP) substituents with the key difference being the oxygen atom in the DTPO group linking it to the Pc core. The influence of four DTP substituents attached to a porphyrin on the self-assembly of such derivatives was extensively investigated by Jung et al.<sup>25</sup> and Buchner et al.<sup>29</sup> The pronounced ability of the DTPO peripheral groups to rotate allows the molecule to adopt different conformations and hence to arrange itself in different ordered patterns that can even coexist on a single substrate, as shown later. More specifically, the DTPO substituents used in this study

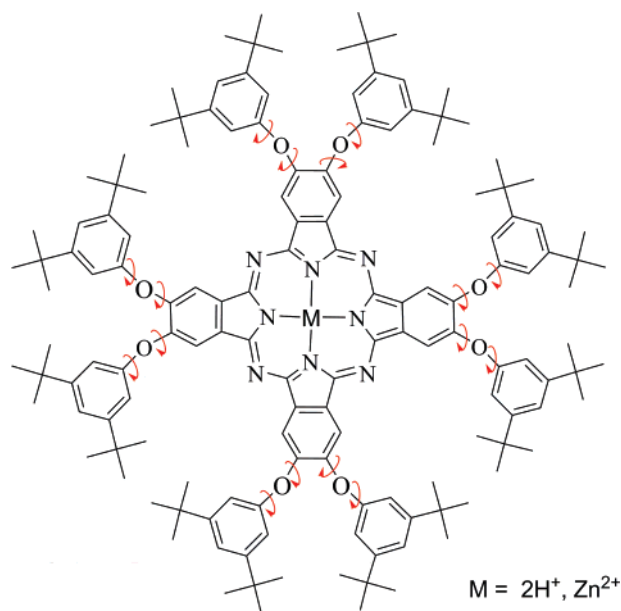
\* To whom correspondence should be addressed. (S.-X.L.) E-mail: liu@iac.unibe.ch. Tel.: +41 31 631 4363. Fax: +41 31 631 3995. (M.S.) E-mail: Meike.Stoehr@unibas.ch. Tel.: +41 61 267 3759. Fax: +41 61 267 3784. (T.J.) E-mail: thomasjung@psi.ch.

<sup>†</sup> University of Basel.

<sup>‡</sup> University of Bern.

<sup>§</sup> Paul-Scherrer-Institute.

**SCHEME 1: Schematic Molecular Structure of the Phthalocyanine Derivative Symmetrically Octasubstituted with Di-(*tert*-butyl)phenoxy (DTPO) Groups<sup>a</sup>**



<sup>a</sup> The two central hydrogen atoms can be replaced by a metal atom being in the oxidation state 2+. The DTPO substituents can rotate around the C—O as well as the O—C bonds as indicated by arrows.

exhibit rotational degrees of freedom that lead to a cone-shaped envelope for all possible conformations of each DTPO substituent including the rotations of the phenyl rings along the O—C bonds. Moreover, there are eight rather than four substituents attached to the Pc core.<sup>18c</sup> Nonetheless, the DTPO groups cannot move independently of each other, as neighboring DTPO groups interfere sterically; therefore, the conformational dynamics is hindered. This is characteristically different to the above-mentioned case of the DTP substituents, because their rotation is only hindered by interaction with the porphyrin core. Consequently, such a flexible, yet complex system of substituents allows for various stable or metastable conformations due to the complex trajectory in conformational space that needs to be followed to reach the most favorable energetic position.

## Experimental Section

All experiments were performed in an ultrahigh vacuum (UHV) system ( $p_{\text{base}} = 2 \times 10^{-10}$  mbar) consisting of different chambers for sample preparation and characterization. Atomically flat Ag(111) and Au(111) samples exhibiting terraces up to 300 nm in width and separated by monatomic steps were prepared by repeated cycles of sputtering with  $Ar^+$  ions and thermal annealing. All molecules were transferred onto the metal surfaces (kept at 298 K) by sublimation from a Knudsen-cell-type evaporator with a deposition rate of about 0.2 ML/min. The rate was checked with a quartz crystal microbalance. After deposition of the molecular layer, a home-built STM operated at room temperature was used to characterize the samples. The measurements were performed in constant-current mode using chemically etched tungsten tips. Typical scan rates were in the range of 2–4 Hz per scan line. The bias voltage was applied to the sample while the tip was grounded.

## Results and Discussion

The self-assembly behavior of ZnPc and H<sub>2</sub>Pc octasubstituted with DTPO groups on Ag(111) and Au(111), respectively, was

studied by STM for molecular coverages less than one monolayer. Figure 1 shows two overview images of the H<sub>2</sub>Pc derivatives deposited on Au(111) and Ag(111), respectively. In total, three different ordered phases were observed, and in each image two of them are present. Figure 1a displays the phases labeled II and III. A well-defined phase boundary between these two specific arrangements runs diagonally across the picture where a single chain of molecules simultaneously participates in each of the two phases. This is expressed by a characteristically different mutual arrangement of the substituents of the Pcs defining the boundary, whereby half of them fit phase II and the other half phase III. Figure 1b displays phases I and III, which are separated by a 2D lattice-gas phase.<sup>13,30</sup> Importantly, within the experimental accuracy the observed phases do not exhibit any differences for both types of Pc derivatives (ZnPc-DTPO and H<sub>2</sub>Pc-DTPO) on both Ag(111) and Au(111) substrates.<sup>31</sup> Therefore, for a more detailed description of the arrangements we will not differentiate between ZnPc-DTPO and H<sub>2</sub>Pc-DTPO, but will refer to both of them as Pc-DTPO.

The three different phases I–III are compared in Figure 2 on the basis of STM data together with their corresponding and most plausible molecular models. For each phase, a 2D unit cell is outlined in red, whereas the unit cell parameters with the resulting surface densities are given in Table 1.

Phase I (Figure 2a,d) exhibits a squarelike unit cell with a lattice constant of  $(3.00 \pm 0.15)$  nm, and the angle between the two lattice vectors is measured at  $(90 \pm 3)^\circ$ . Consequently, the distance between adjacent molecules would allow some conformational flexibility for the eight DTPO substituents. However, due to steric hindrance between *tert*-butyl groups<sup>26</sup> belonging to neighboring DTPO substituents, a conformation of the DTPO groups for which the phenyl rings are totally coplanar with the substrate surface cannot occur. Hence, the DTPO groups are slightly tilted and are above the plane of the Pc core. The bright lobes in Figure 2a correspond most likely to the topmost *tert*-butyl groups that are closest to the center of the molecule. Phase I exhibits the lowest surface density of molecules ( $\approx 0.11$  molecules per nm<sup>2</sup>) of all three phases, and it is observed with the lowest probability.

In phase II (Figure 2b,e), the Pc-DTPO molecules are arranged in a rhombic geometry with axes of  $(2.5 \pm 0.13)$  nm in length and an angle of  $(67 \pm 3)^\circ$ . The distance between adjacent molecules is clearly smaller than in phase I, which can be explained by a distinct out-of plane conformation of the DTPO groups (visible as bright lobes in Figure 2b), enabling a side-to-side packing of two DTPO groups attached to the same benzo-ring of the Pc core (Figure 2e). Overall, the Pc-DTPO molecule forms a crosslike shape, which considerably reduces the space required for all the DTPO groups. Consequently, the surface density of the molecules increases to ca. 0.17 molecules per nm<sup>2</sup>. Phase II is observed with a considerably higher probability than phase I.

In phase III (Figure 2c), the Pc-DTPO molecules are arranged in an oblique symmetry described by a rhomboid with axes of  $(2.5 \pm 0.13)$  and  $(2 \pm 0.1)$  nm in length and an angle of  $(73 \pm 3)^\circ$ . This arrangement can be conceived as if the entire rows of Pc-DTPOs in phase II along the unit cell axis *a* would be squeezed together approximately in the direction of the axis *b* (Figure 2e). Such a compression results into a shortening of the unit cell axis *b* (see model in Figure 2f, Table 1) and additionally into the highest observed surface density of all three ordered phases ( $\approx 0.21$  molecules per nm<sup>2</sup>). On the whole, a more complex conformation of the DTPO substituents is



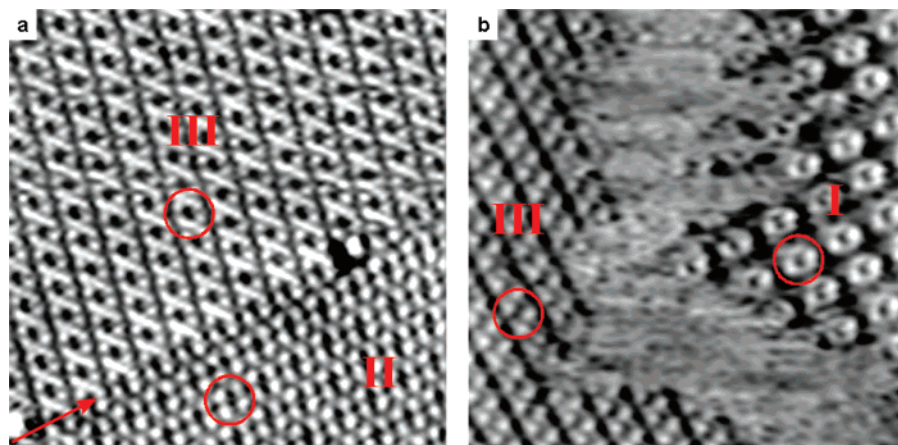


**Figure 1.** The two large scale STM images show the three ordered phases labeled I– III and a coexisting gas-phase found for the  $\text{H}_2\text{Pc-DTPO}$  molecules on both  $\text{Ag}(111)$  and  $\text{Au}(111)$ , respectively. Image in panel a ( $60 \times 60 \text{ nm}^2$ , 7 pA, 2.5 V) shows the phases labeled II and III on  $\text{Au}(111)$ . Merging of the two phases is clearly visible, and the single chain of molecules defining the phase boundary and participating simultaneously in both phases is marked by an arrow. Image in panel b ( $60 \times 60 \text{ nm}^2$ , 10 pA,  $-2.1 \text{ V}$ ) displays phases I and III separated by a gas phase on  $\text{Ag}(111)$ . In both images, an individual molecule in each of the phases I, II, and III is highlighted by a red circle.

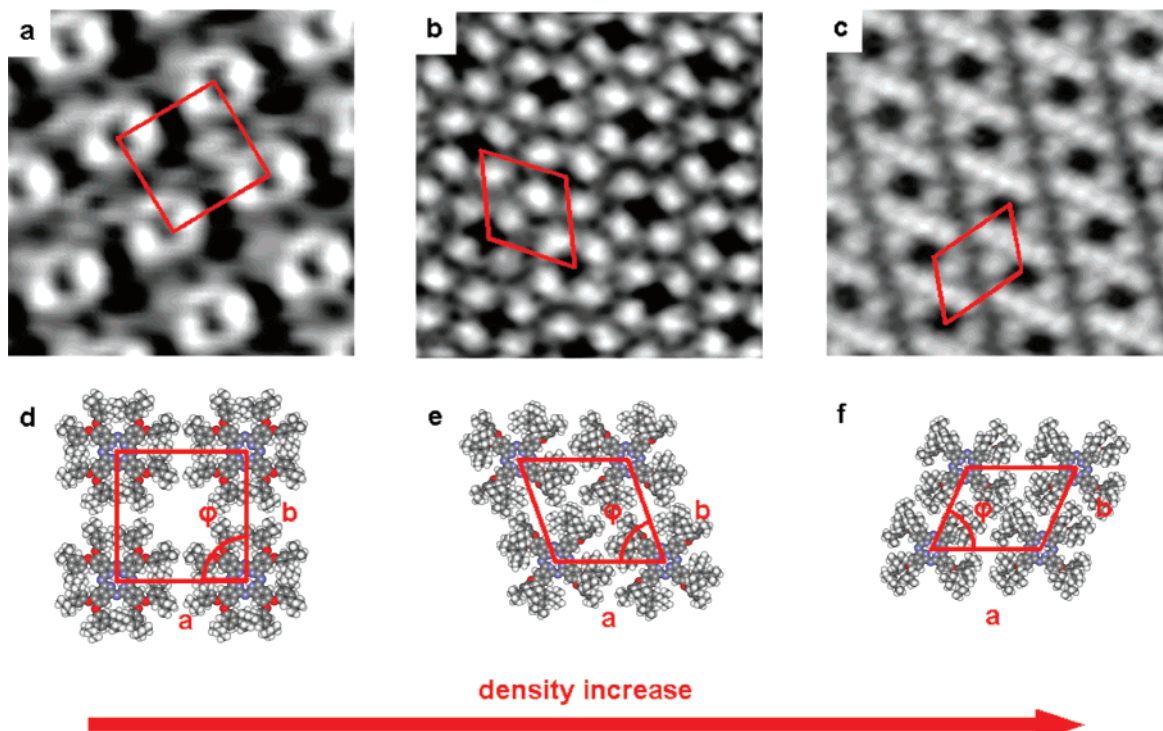


**Figure 2.** (a–c) Each STM image ( $10 \times 10 \text{ nm}^2$ ) shows in detail one of the three different ordered phases found for the  $\text{Pc-DTPOs}$ : (a) phase I on  $\text{Au}(111)$  (7 pA, 2.3 V); (b) phase II on  $\text{Au}(111)$  (7 pA, 2.5 V); (c) phase III on  $\text{Ag}(111)$  (10 pA,  $-2.1 \text{ V}$ ). (d–f) Corresponding models for the observed phases I, II, and III, respectively. The 2D unit cells are drawn in red (corresponding parameters are given in Table 1).

**TABLE 1: Parameters of the Unit Cells Corresponding to Phases I, II, and III and Their Surface Densities**

phase	$a[\text{nm}]$	$b[\text{nm}]$	$\varphi[^\circ]$	$\rho[\text{molecules}/\text{nm}^2]$
I	$3 \pm 0.15$	$3 \pm 0.15$	$90 \pm 3$	0.11
II	$2.5 \pm 0.13$	$2.5 \pm 0.13$	$67 \pm 3$	0.17
III	$2.5 \pm 0.13$	$2 \pm 0.1$	$73 \pm 3$	0.21

required for this arrangement, but it cannot be identified only on the basis of Figure 2c. However, changing the scanning conditions allowed us to acquire an alternative view of the  $\text{Pc-DTPO}$  molecules<sup>32</sup> and in turn to deduce a tentative model (Figure 2f). The image in Figure 3 represents this view of phase III superimposed by a color image of the same phase depicted as in Figure 2c only with an enhanced contrast. Although in Figure 2c six bright lobes per  $\text{Pc-DTPO}$  molecule are visible, Figure 3 reveals the  $\text{Pc}$  core itself (appearing as a gray cross

with a characteristic dark spot in the center that we associate with the central metal atom in analogy to earlier studies by Hipps et al.<sup>4,6</sup>) that is surrounded by fourteen bright lobes, ten of which belong to the same  $\text{Pc-DTPO}$  molecule. From the superposition of the images, it can be deduced that the six lobes from Figure 2c do not correspond to any of the ten lobes underneath, making altogether sixteen separate lobes. In agreement with the characteristic appearance of the tert-butyl groups of DTP substituents (discussed in references in some detail),<sup>25,26</sup> each of the bright spots can be assigned to one of the sixteen tert-butyl groups of our  $\text{Pc}$  derivative. Therefore, we can assume that Figure 2c shows the six topmost tert-butyl groups belonging to the six  $\text{DTPO}$  substituents rotated completely out of plane, and Figure 3 shows the  $\text{Pc}$  core and ten tert-butyl groups positioned in closer proximity to the substrate surface. Four of

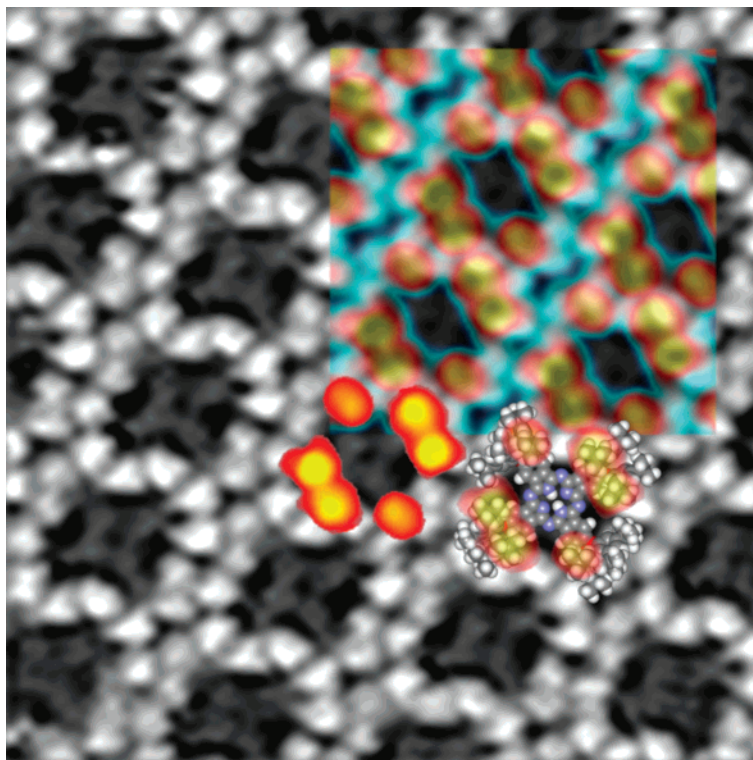


**Figure 3.** High-resolution STM image ( $10 \times 10 \text{ nm}^2$ , 63 pA, 0.8 V) featuring an alternative view of Pc-DTPOs on Ag(111) self-assembled in phase III (in black and white). A false-color image of a typical view of phase III (as depicted in Figure 2c) is superimposed. In addition, a tentative model of the Pc-DTPO is drawn.

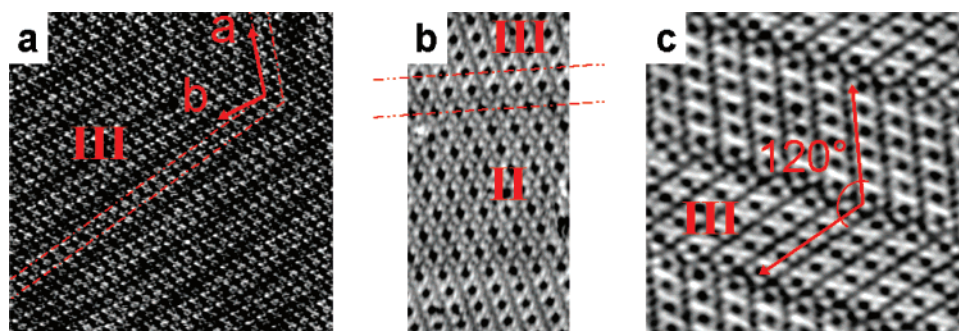


**Figure 4.** (a) STM image ( $50 \times 50 \text{ nm}^2$ , 8 pA, 2.1 V) of Pc-DTPOs on Au(111) self-assembled in phase III. The reconstruction of the underlying Au(111) surface is visible in superposition to the molecular contrast. It is highlighted by two dotted lines. The unit cell vectors, linearly magnified by a factor 4, are shown. Vector *a* is parallel to the reconstruction, whereas vector *b* is deflected by  $\approx 12^\circ$ . (b) STM image ( $37 \times 18 \text{ nm}^2$ , 7 pA, 2.1 V) of phases II and III on Au(111). The dotted lines above and below the phase boundary indicate the parallel orientation of the unit cell vectors in both phases. (c) STM image ( $25 \times 25 \text{ nm}^2$ , 7 pA, 2.5 V) showing different domains of phase III on Au(111), exhibiting different orientations.

the lobes correspond to two DTPO substituents oriented almost coplanar with the Pc core, whereas the remaining six lobes correspond to the lower counterparts of the topmost tert-butyl groups, seen in Figure 2c. Furthermore, through the rotation of these six DTPO substituents into an out-of-plane orientation, a side-by-side packing of the DTPO substituents belonging to adjacent Pc-DTPO molecules is enabled. Because of steric constraints, this compression is only possible in one direction. Thus, as can be seen in Figure 3, in one direction double rows are formed by six bright lobes between two adjacent molecules (three lobes per molecule), whereas in the other direction single rows of four bright spots in fairly linear alignment are visible. In a single row, two neighboring lobes belong to one and the other two lobes to the other molecule. These four lobes correspond to side-by-side packed DTPO groups. This model, derived from the STM data, is consistent with the above-mentioned squeezing of the rows of Pc-DTPOs. Altogether, phase III is associated with a denser packing of the DTPO

groups, which in turn reflects an increase in the surface density of the Pc-DTPOs and in the interaction between nearest neighbors, although at the same time it puts constraints on their conformations. The probability to observe phase III is by far the highest for all phases. It is noteworthy that it is the only phase remaining after annealing at  $150^\circ\text{C}$ .

The orientation of the molecular assemblies of phases II and III with respect to the substrate can be derived from the STM images exhibiting both the known Au(111) reconstruction<sup>33</sup> and molecular resolution (Figure 4a). From Figure 4a, it can be deduced that the unit cell vector *a* is parallel to the  $[11\bar{2}]$  direction. As seen in Figure 4b, vector *a* of phase III is always parallel to one of the vectors of phase II (*a* and *b* are of equivalent length). Therefore, also one of the vectors of phase II is parallel to the  $[11\bar{2}]$  direction. Because of the 3-fold symmetry of both the Au(111) and the Ag(111) surface, phase III exhibits three possible orientations with an angle of  $120^\circ$  (Figure 4c). On the other hand, phase II exists in six possible



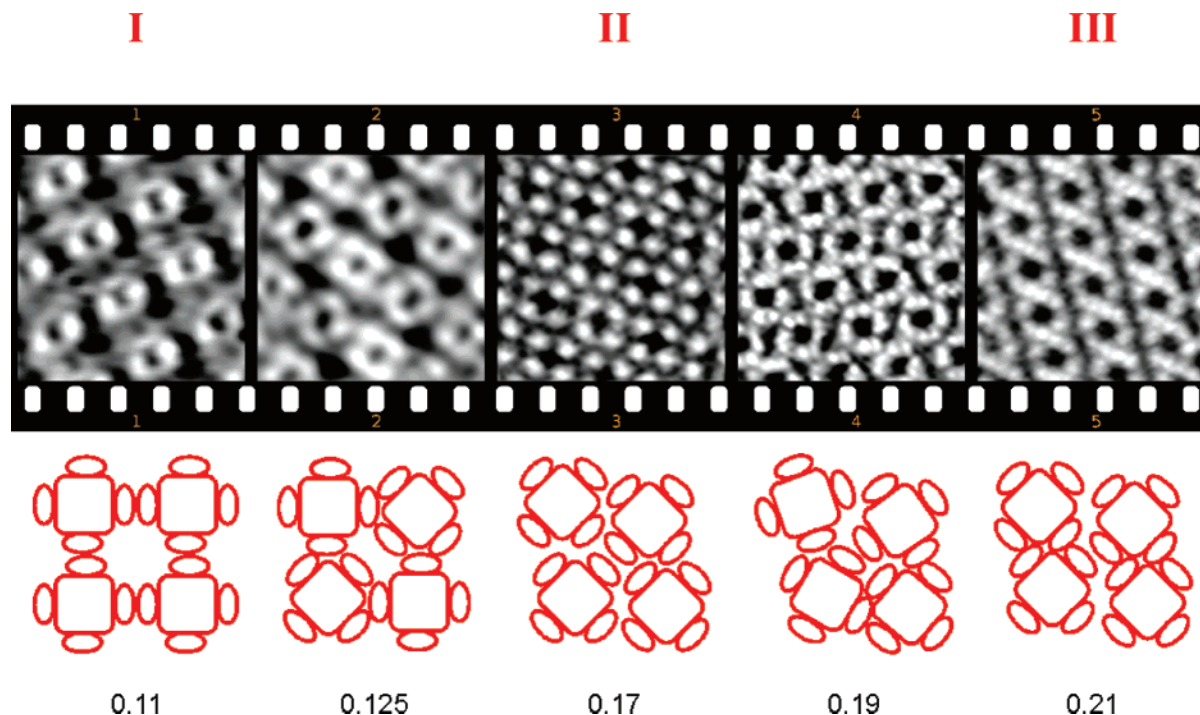


**Figure 5.** Sequence of five STM images of  $10 \times 10 \text{ nm}^2$ . Images 1, 3, and 5 correspond to the STM images in Figure 2a–c and depict phases I, II, and III, respectively. Image 2 shows a transient phase between phases I and II on Au(111) (7.4 pA, 1.2 V). Image 4 shows a transient phase between phases II and III on Ag(111) (8 pA, 3 V). Simplified models of the corresponding phases are shown in the cartoons below, together with corresponding approximate densities in molecules per  $\text{nm}^2$ .

orientations with an angle of  $60^\circ$ , because its unit cell vectors are of equivalent length. No correlation of the orientation of phase I to other phases or to the substrate lattice was observed.

Another point is that because of the steric entanglement between neighboring DTPO substituents, complex trajectories in conformational space are required to reorient the substituents into conformations characteristic for the above-described phases. This indicates significant retardation of the thermodynamic optimization of the conformations. Also, the proximity of the delocalized  $\pi$ -system of the Pc core to the metal substrate enables a considerable attractive Pc–metal interaction (comparable to unsubstituted phthalocyanine adsorbates)<sup>34</sup> and consequently reduces the conformational space of the DTPO substituents. To fully exploit the rotational degrees of freedom of the phenoxy link on account of a conformational optimization, an increase of the distance between the Pc core and the metal substrate would be necessary. This, however, would require additional energy to overcome the attractive Pc–metal interaction.

Interestingly, the conformational evolution allows for sporadic observations of transient states between the comparatively stable phases I, II, and III (Figure 5). Presumably because of the Pc–metal interaction, organizations with higher surface densities are observed with a higher probability because they allow more Pc cores to interact with the substrate. Hence, stable phases can be considered as local minima of the total energy of the system with phase I being the highest minimum of all phases and phase III being the global minimum. The global minimum can be reached by providing thermal energy to the system for a sufficient amount of time. This is in agreement with the above-mentioned observation of phase III as the only remaining phase upon annealing at  $150^\circ\text{C}$ .

The orientation of the unit cell vectors of phases II and III, which are parallel to the [112] direction of the substrate, might signify the influence of the substrate lattice on the assembly of the Pc-DTPOs. Nonetheless, the fact that the reconstruction of

the underlying Au(111) surface remains intact and that there is no orientational correlation of phase I to the substrate lattice indicates that the interaction of the Pc core with the metal substrate (physisorption) is minor compared to other factors. Hence, from our model we conclude that the featured multiphase behavior is mainly induced by (i) the manifold of conformations of the DTPO substituents, (ii) their steric entanglement, and (iii) the energy gain associated with the increased surface density of the Pc cores interacting with the metal substrate.

## Conclusions

Peripheral DTPO substituents of Pc-DTPO molecules influence and dictate the type of self-assembly within their molecular layers on Au(111) and Ag(111) substrates, respectively. Thereby, several ordered phases of different symmetries and surface densities emerge. These phases coexist due to the retardation of the conformational optimization in consequence of the steric entanglement of the substituents. In addition, the phenoxy group remarkably increases the conformational possibilities of the substituted Pc molecules. The additional rotational degrees of freedom induced by the oxygen atom linking each DTPO substituent to the Pc core allow all the substituents to be arranged above the plane of the Pc core, forming a bowl-like structure, which enables the interaction of the Pc core with the metal substrate. This is in clear contrast to the conformational possibilities of porphyrins substituted with DTP groups. There, the interaction of the central part of the molecule with the substrate is more hindered, because the DTP groups prevent the central part to be positioned in close proximity to the substrate.<sup>26</sup>

There is now considerable evidence that the stability, the well-defined ordering and the bowl-like shape of the specific Pc derivatives arranged within these phases, predetermine such systems as a potential host for other guest molecules to construct novel surface architectures. The hosting properties of these systems are currently under investigation.

**Acknowledgment.** We thank the Swiss National Science Foundation (Grants 200020-116003 and 200020-117610), the National Centre of Competence in Research (NCCR) “Nanoscale Science” and the European Union (RTN Network PRAIRIES; MRTN-CT-2006-035810) for funding. M.S. acknowledges support from the German Academy of Natural Scientists Leopoldina under the Grant BMBF-LPD 9901/8-86. S. Schnell is gratefully acknowledged for his valuable assistance with the experimental setup and the sample preparation procedures. Furthermore, we acknowledge the continuous support of Professor H.-J. Güntherodt. We also thank Nanonis Inc. for the fruitful collaboration on the data acquisition system.

**Supporting Information Available:** STM images as referenced. This information is available free of charge via the Internet at <http://pubs.acs.org>.

## References and Notes

- (1) Leznoff, C. C.; Lever, A. B. P. *Phthalocyanines: Properties and Applications*; VCH: Weinheim, 1996; Vols. 1–4.
- (2) Kadish, K. M.; Smith, K. M.; Guillard, R. *The Porphyrin Handbook*; Academic Press: San Diego, CA, 2003; Vols. 1–14.
- (3) de la Torre, G.; Claessens, C. G.; Torres, T. *Chem. Commun.* **2007**, 20, 2000.
- (4) Lu, X.; Hipps, K. W.; Wang, X. D.; Mazur, U. *J. Am. Chem. Soc.* **1996**, *118*, 7197.
- (5) Hipps, K. W.; Lu, X.; Wang, X. D.; Mazur, U. *J. Phys. Chem.* **1996**, *100*, 11207.
- (6) Lu, X.; Hipps, K. W. *J. Phys. Chem. B* **1997**, *101*, 5391.
- (7) Barlow, D. E.; Hipps, K. W. *J. Phys. Chem. B* **2000**, *104*, 5993.
- (8) Grand, J.-Y.; Kunstmann, T.; Hoffmann, D.; Haas, A.; Dietsche, M.; Seifritz, J.; Möller, R. *Surf. Sci.* **1996**, *366*, 403.
- (9) Lackinger, M.; Hietschold, M. *Surf. Sci.* **2002**, *520*, L619.
- (10) Yoshimoto, S.; Tada, A.; Suto, K.; Itaya, K. *J. Phys. Chem. B* **2003**, *107*, 5836.
- (11) Suto, K.; Yoshimoto, S.; Itaya, K. *J. Am. Chem. Soc.* **2003**, *125*, 14976.
- (12) Yoshimoto, S.; Tsutsumi, E.; Suto, K.; Honda, Y.; Itaya, K. *Chem. Phys.* **2005**, *319*, 147.
- (13) Berner, S.; Brunner, M.; Ramoino, L.; Suzuki, H.; Güntherodt, H.-J.; Jung, T. A. *Chem. Phys. Lett.* **2001**, *348*, 175.
- (14) Mannsfeld, S.; Reichhard, H.; Fritz, T. *Surf. Sci.* **2003**, *525*, 215.
- (15) Lackinger, M.; Müller, T.; Gopakumar, T. G.; Müller, F.; Hietschold, M.; Flynn, G. W. *J. Phys. Chem. B* **2004**, *108*, 2279.
- (16) Gopakumar, T. G.; Müller, F.; Hietschold, M. *J. Phys. Chem. B* **2006**, *110*, 6060.
- (17) (a) Gearba, R. I.; Bondar, A. I.; Goderis, B.; Bras, W.; Ivanov, D. A. *Chem. Mater.* **2005**, *17*, 2825. (b) Kroon, J. M.; Kochorst, R. B. M.; van Dijk, M.; Sanders, G. M.; Sudhölter, E. J. R. *J. Mater. Chem.* **1997**, *7*, 615.
- (18) (a) Hatsusaka, K.; Ohta, K.; Yamamoto, I.; Shirai, H. *J. Mater. Chem.* **2001**, *11*, 423. (b) Haas, M.; Liu, S.-X.; Neels, A.; Decurtins, S. *Eur. J. Org. Chem.* **2006**, *24*, 5467. (c) Haas, M.; Liu, S.-X.; Kahnt, A.; Leiggener, C.; Guldi, D. M.; Hauser, A.; Decurtins, S. *J. Org. Chem.* **2007**, *72*, 7533.
- (19) (a) Donders, C. A.; Liu, S.-X.; Loosli, C.; Sanguinet, L.; Neels, A.; Decurtins, S. *Tetrahedron* **2006**, *62*, 3543. (b) Loosli, C.; Jia, C.; Liu, S.-X.; Haas, M.; Dias, M.; Levillain, E.; Neels, A.; Labat, G.; Hauser, A.; Decurtins, S. *J. Org. Chem.* **2005**, *70*, 4988.
- (20) Qiu, X. H.; Wang, C.; Zeng, Q. D.; Xu, B.; Yin, S. X.; Wang, H. N.; Xu, S. D.; Bai, C. L. *J. Am. Chem. Soc.* **2000**, *122*, 5550.
- (21) Abel, M.; Oison, V.; Koudia, M.; Maurel, C.; Katan, C.; Porte, L. *ChemPhysChem* **2006**, *7*, 82.
- (22) Koudia, M.; Abel, M.; Maurel, C.; Blik, A.; Catalin, D.; Mossoyan, M.; Mossoyan, J.-C.; Porte, L. *J. Phys. Chem. B* **2006**, *110*, 10058.
- (23) Oison, V.; Koudia, M.; Abel, M.; Porte, L. *Phys. Rev. B* **2007**, *75*, 035428.
- (24) Liu, A. Z.; Lei, S. B. *Surf. Interface Anal.* **2007**, *39*, 33.
- (25) Jung, T. A.; Schlittler, R. R.; Gimzewski, J. K. *Nature* **1997**, *386*, 696.
- (26) Yokoyama, T.; Kamikado, T.; Yokoyama, S.; Mashiko, S. *J. Chem. Phys.* **2004**, *121*, 11993.
- (27) Katsonis, N.; Vicario, J.; Kudernac, T.; Visser, J.; Pollard, M. M.; Feringa, B. L. *J. Am. Chem. Soc.* **2006**, *128*, 15537.
- (28) Auwärter, W.; Weber-Bargioni, A.; Riemann, A.; Schiffrin, A.; Gröning, O.; Fasel, R.; Barth, J. V. *J. Chem. Phys.* **2006**, *124*, 194708.
- (29) Buchner, F.; Comanici, K.; Jux, N.; Steinrück, H.-P.; Marbach, H. *J. Phys. Chem. C* **2007**, *111*, 13531.
- (30) See supporting information (Figure 1).
- (31) See supporting information (Figure 2).
- (32) See supporting information (Figure 3).
- (33) Barth, J. V.; Brune, H.; Ertl, G.; Behm, R. *J. Phys. Rev. B* **1990**, *42*, 9307.
- (34) Witte, G.; Wöll, C. *J. Mater. Res.* **2004**, *19*, 1889.